Efficient Integral Equation Approach for the Modelling of Glide-Symmetric Structures

Efficient Integral Equation Approach for the Modelling of Glide-Symmetric Structures

M. Petek*, J. Rivero*, J. A. Vasquez-Tobon*, G. Valerio†‡, O. Quevedo-Teruel§, F. Vipiana*
*Dept. of Electronics and Telecommunications, Politecnico di Torino, 10129, Torino, Italy
{martin.petek, javier.rivero, jorge.tobon, francesca.vipiana}@polito.it
†Sorbonne Université, CNRS, Laboratoire de Génie Électrique et Électronique de Paris (GeePs), 75252, Paris, France
‡Université Paris-Saclay, CentraleSupélec, CNRS, GeePs, 91192, Gif-sur-Yvette, France
§KTH Royal Institute of Technology, Division of Electromagnetic Engineering, 11428, Stockholm, Sweden

***Abstract*—For the design of advanced microwave and antenna components, efficient and accurate electromagnetic methods are required. In this work, we present a technique to fast simulate mirror- and glide-symmetric periodic structures. More concretely, a novel Green's function is proposed which allows to reduce the computational domain to one half of the unit cell. Full dispersion diagrams are computed for metallic glide- and mirror-symmetric structures with three stages of mesh refinement. The results converge with the meshing and agree well with conventional eigenmode analyses.**

***Index Terms*—Glide symmetry, integral equations, dispersion diagram, periodic structures, metamaterials.**

I. Introduction

Recently, a renewed interest in higher symmetries, and especially glide symmeries, has raised in the microwave community [1], [2]. One of the most interesting features of glide symmetries is their capacity to increase the bandwidth of operation. A periodic structure is considered to be glide-symmetric if it is invariant with respect to a translation by half a period and mirroring [3], [4]. In glide-symmetric structures, the first stopband is closed thus reducing dispersion and increasing the operational bandwidth of the structure. This property has been successfully applied for the design of broadband lenses [5], [6]. In addition, glide symmetries are able to increase the bandwidth of the stopband in metallic holey structures. This property has been applied for the design of filters [7], and to reduce leakage in interconnections [8], [9]. Glide symmetries have also been applied to leaky wave antennas [10].

To the authors' knowledge, the available commercial solvers are unable to calculate attenuation in the stopband. To remedy this, an ad hoc method called multi-modal transfer matrix method (MMTMM) [11] was recently proposed. This is a hybrid method where the coupling between different port modes placed at the edges of the unit cell is obtained by a full wave solver. Then, the dispersion diagram can be computed through a post-processing procedure. The approach can be used to obtain attenuation in stopbands and complex modes of lossy unit cells. Alternatively, mode matching has been proposed in [12] for the analysis of glide-symmetric unit cells. In this technique, fields are expanded into modes which couple in such a way that boundary conditions are satisfied at the discontinuities. This technique is numerically very efficient, especially if the modes of the structure can be found analytically, but it is more difficult to implement when the structure geometry is complex.

In this paper, we present an alternative modelling approach based on solving the electric field integral equation with method of moments. We extend the work presented in [13], [14] by introducing a novel Green's function which allows us to only compute interactions in half of the unit cell by exploiting the symmetry of the structure. The proposed approach can compute dispersion diagrams and the attenuation in the stopbands and can be extended to include lossy metals.

II. Method of moments formulation

The surfaces in the structure are described with a perfect electric conductor. Thus, the relationship between scattered field and incident field is:

$$-\mathbf{E}^i_{\tan}(\mathbf{r}) = \mathbf{E}^s_{\tan} = -j\omega\mathbf{A} - \nabla\Phi, \tag{1}$$

where the scattered field is further split into vector and scalar potentials. These can be computed by integration over the scatterer S:

$$\mathbf{A} = \int_S \mathbf{J}(\mathbf{r}')G(\mathbf{r},\mathbf{r}')\,\mathrm{d}S' \tag{2}$$

$$\Phi = -\frac{1}{j\omega\varepsilon}\int_S \nabla'\cdot\mathbf{J}(\mathbf{r}')G(\mathbf{r},\mathbf{r}')\,\mathrm{d}S', \tag{3}$$

where ε is the permittivity, ω is the angular frequency, $\mathbf{J}(\mathbf{r}')$ is the surface current density which is unknown and $G(\mathbf{r},\mathbf{r}')$ is a Green's function. The unprimed and primed vectors $\mathbf{r}$ and $\mathbf{r}'$ are the observation and the source points. As the structure is infinitely periodic, the computational domain can be restricted to a single unit cell if a periodic Green's function is defined. For fully metallic structures, the free-space periodic Green's function (FSPGF) [15] is used to allow for efficient simulation of a single unit cell. The FSPGF is a doubly infinite sum of free-space Green's functions where the sources radiate with different phases depending on transverse wave vector $\mathbf{k}_{\mathrm{t}00}$. For closed structures we can interpret $\mathbf{k}_{\mathrm{t}00}$ as the wave vector of the mode in the bounded structure. The FSPGF is then given by:

$$G(\mathbf{r},\mathbf{r}') = \sum_{m=-\infty}^{\infty}\sum_{n=-\infty}^{\infty} G_{mn}, \tag{4}$$

where

$$G_{mn} = e^{-j\mathbf{k}_{\mathrm{t}00}\cdot\rho_{mn}} \frac{e^{-jkR_{mn}}}{4\pi R_{mn}}. \quad (5)$$

Here, $\rho_{mn} = m\mathbf{s}_1 + n\mathbf{s}_2$ is the distance vector from the origin to the point at m, n in the lattice, $\mathbf{s}_1$ and $\mathbf{s}_2$ are the lattice periodicities, and $R_{mn} = \sqrt{(z-z')^2 + |\rho - \rho' - \rho_{mn}|^2}$ is the distance from the source point at m, n to the observation point. As an extension of (4), we introduce a Green's function designed to more efficiently model structures with either mirror or glide symmetry. In both cases, the wave propagates between two parallel plates which are symmetric with respect to a mirror in z and in the case of glide symmetry a translation of

$$\rho_g = 0.5\mathbf{s}_1 + 0.5\mathbf{s}_2 \quad (6)$$

in x and y is added. The Green's function is constructed by adding together two FSPGF, a real Green's function and an image Green's function, into a higher-symmetric periodic Green's function (HSPGF):

$$G(\mathbf{r}, \mathbf{r}') = \sum_{m=-\infty}^{\infty} \sum_{n=-\infty}^{\infty} G_{mn} \pm e^{-j\mathbf{k}_{\mathrm{t}00}\cdot\rho_g} G_{mn,t}, \quad (7)$$

where G_{mn} is taken from (5), $\rho_g = \mathbf{0}$ for the mirror symmetry, and $G_{mn,t}$ is obtained by replacing

$$R_{mn} \to R_{mn,\mathrm{t}} = \sqrt{(z+z')^2 + |\rho - \rho' - \rho_{mn} - \rho_g|^2} \quad (8)$$

into (5). Depending on whether the fields are mirrored by perfect electric conductor or perfect magnetic conductor, the values in (7) are subtracted or summed. Similarly to the FSPGF, the equation presented in (7) suffers from extremely slow convergence. By splitting the sum into spatial and spectral parts [16], [17], we can achieve a Gaussian convergence by setting the value of the splitting parameter to

$$E = \sqrt{\frac{\pi}{A}}, \quad (9)$$

where A is the area of the unit cell. However, when the size of the unit cell is comparable to the wavelength, the value of the splitting parameter must be adjusted to ensure numerical stability at the cost of slower convergence [18]. The Ewald's method, along with the procedure for proper selection of the splitting parameter E, is done separately for both series of G_{mn} and $G_{mn,t}$.

In order to obtain a system of equations we employ a procedure known as method of moments [19]. The surface S is first discretized with a triangular mesh and the current in the expressions for potentials (2) and (3) is expanded into

$$\mathbf{J}(\mathbf{r}) = \sum_{n=1}^{N} I_n \mathbf{\Lambda}_n(\mathbf{r}), \quad (10)$$

where $\mathbf{\Lambda}_n(\mathbf{r})$ are RWG basis functions [20] and I_n are the coefficients of the surface current density to be obtained. Note that when the mirroring operation is done, it is necessary to change the sign of the z component of $\mathbf{\Lambda}_n$. Furthermore, additional triangles are placed at the edge of the unit cell to ensure current continuity [13], [14]. Then, the Galerkin testing procedure is used to obtain a system of equations:

$$\mathbf{ZI} = \mathbf{V}, \quad (11)$$

where $\mathbf{Z}$ is the impedance matrix, $\mathbf{I}$ is a vector of current coefficients I_n, and $\mathbf{V}$ is a zero vector as no external excitation is needed for modes in the structure to exist. The elements in the impedance matrix $\mathbf{Z}$ are computed by

$$Z_{mn} = j\omega L_{mn} + \frac{1}{j\omega} S_{mn}, \quad (12)$$

where

$$L_{mn} = \mu \int_S \mathrm{d}S \mathbf{\Lambda}_m(\mathbf{r}) \cdot \int_S \mathrm{d}S' \mathbf{\Lambda}_n(\mathbf{r}') G(\mathbf{r}, \mathbf{r}') \quad (13)$$

and

$$S_{mn} = \frac{1}{\varepsilon} \int_S \mathrm{d}S \nabla \cdot \mathbf{\Lambda}_m(\mathbf{r}) \int_S \mathrm{d}S' \nabla' \cdot \mathbf{\Lambda}_n(\mathbf{r}') G(\mathbf{r}, \mathbf{r}'). \quad (14)$$

Equations (13) and (14) require a careful treatment of the integrals, as they are singular when $m = n$. In this work, we use a singularity cancellation scheme for singular and near-singular elements to ensure an accurate computation [21].

The obtained system of equations can be solved by finding the value of parameter $\mathbf{k}_{\mathrm{t}00}$ such that the determinant of the matrix $\mathbf{Z}$ is exactly zero:

$$\det(\mathbf{Z}(\mathbf{k}_{\mathrm{t}00})) = 0. \quad (15)$$

In practice, this condition is never exactly obtained due to finite precision of the elements in $\mathbf{Z}$. Thus, we must find all values of $\mathbf{k}_{\mathrm{t}00}$ for which the determinant of the matrix is at a local minimum. As the determinant is very small, it is usually not representable in a 64-bit floating point number. Instead, the logarithm of the determinant is computed and minimized.

III. Simulation results

For testing, we choose to analyze a rectangular hole structure, as shown in Fig. 1 and represented in the insets of Fig. 2 for the mirror-symmetric case and in Fig. 3 for the glide-symmetric case. However, since HSPGF is used, only the bottom half of the structure is meshed at varius stages of refinement, as shown in Fig. 1. The geometric parameters of the unit cell are indicated in Tab. I. This geometry was chosen as an initial test as it can be perfectly described with flat mesh elements. Since the unit cells are both symmetric in x and y axes and additionally with respect to a 90° rotation, the irreducible Brillouin zone is Γ-X-M-Γ. Thus, the full dispersion diagram can be obtained by varying the phase shifts $\varphi_{x,y}$ over the unit cells

$$\varphi_x = \mathbf{k}_{\mathrm{t}00} \cdot \hat{\mathbf{x}} p_x \quad , \quad \varphi_y = \mathbf{k}_{\mathrm{t}00} \cdot \hat{\mathbf{y}} p_y \quad (16)$$

based on which region of the irreducible Brillouin zone we want to compute:

- Γ-X: $\varphi_x \in [0, \pi]$, $\varphi_y = 0$
- X-M: $\varphi_x = \pi$, $\varphi_y \in [0, \pi]$
- M-Γ: $\varphi_x \in [\pi, 0]$, $\varphi_y = \varphi_x$

The results for mirror- and glide-symmetric structures are plotted in Fig. 2 and in Fig. 3. In both cases, the results agree well with the CST Studio Suite®'s eigenvalue solver (CST ES) and converge with mesh refinement. Furthermore, the accuracy of the simulation can be observed to experience only mild degradation, even when sizes of the largest triangles in the mesh are comparable to a fifth of wavelength.

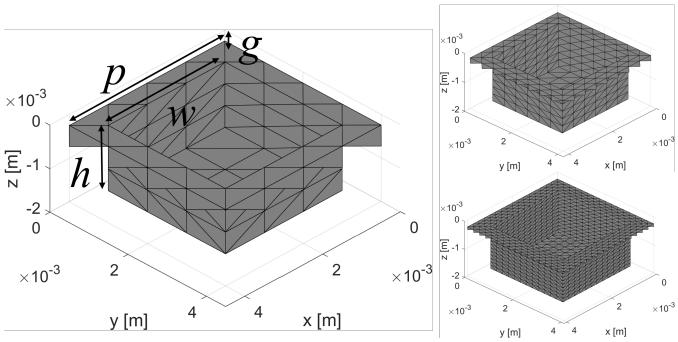

Fig. 1. Refining of the mesh. The largest triangle lengths at 60 GHz are $\lambda/3.5$ (left), $\lambda/7$ (top right), $\lambda/14$ (bottom right), with λ the wavelength. Here, number of the unknowns (basis functions) is $N = 177$, $N = 708$ and $N = 2832$.

TABLE I
GEOMETRIC PARAMETERS FOR THE UNIT AND THE VALUES USED FOR THE SIMULATIONS IN FIGS. 2 AND 3.

Property	Parameter	Value [mm]
period (in x and y)	p	4
hole width	w	3
hole depth	h	1.8
gap	g	0.5

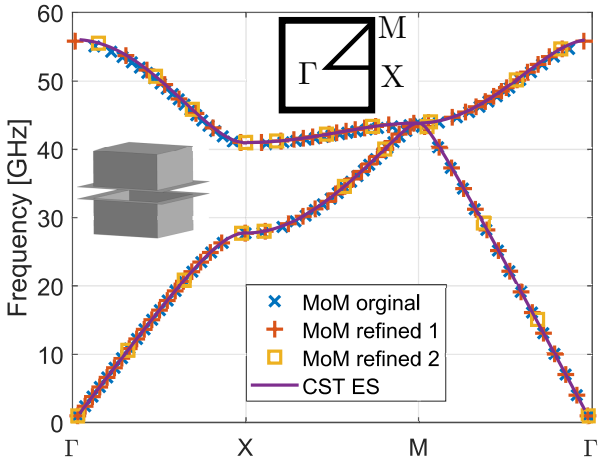

Fig. 2. Dispersion diagram for the mirror-symmetric structure. The dimensions are indicated in Tab. I. The irreducible Brillouin zone and the unit cell are depicted in the insets.

IV. Conclusion and Future Work

We have presented a modelling procedure for accurate computation of dispersion diagrams of mirror-and glide-symmetric structures. The mesh is shown to be converging and the results have a good agreement with the eigenmode analysis of commercial software. The developed technique can be used to study non-canonical shapes of unit cells and to obtain attenuation in the stopband.

In the future, we plan to further test and verify the code, especially for attenuation in the stopband. Furthermore, we wish to further accelerate the method by parallelization of filling the impedance matrix elements and efficiently interpolating the Green's function as proposed in [22].

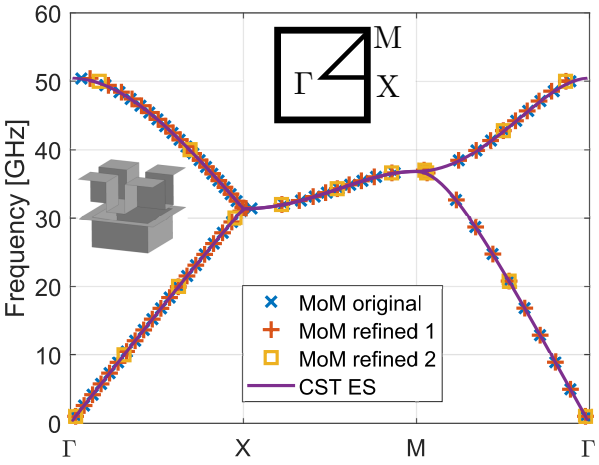

Fig. 3. Dispersion diagram for the glide-symmetric structure. The dimensions are indicated in Tab. I. The irreducible Brillouin zone and the unit cell are depicted in the insets.

Acknowledgment

This publication is based upon work from COST Action Symat (CA18223), supported by COST (European Cooperation in Science and Technology), by the Horizon Europe Research and Innovation Program under the GENIUS Project, Marie Skłodowska-Curie Grant under Agreement 101072560, and in part by the project PON Research and Innovation "Microwave Imaging and Detection powered by Artificial Intelligence for Medical and Industrial Applications (DM 1062/21)," funded by the Italian Ministry of University and Research (MUR). It is also supported by Unite! – University Network for Innovation, Technology and Engineering.

References

[1] O. Quevedo-Teruel, Q. Chen, F. Mesa, N. J. Fonseca, and G. Valerio, "On the benefits of glide symmetries for microwave devices," *IEEE Journal of Microwaves*, vol. 1, no. 1, pp. 457–469, 2021.

[2] O. Quevedo-Teruel, G. Valerio, Z. Sipus, and E. Rajo-Iglesias, "Periodic structures with higher symmetries: Their applications in electromagnetic devices," *IEEE Microwave Magazine*, vol. 21, no. 11, pp. 36–49, 2020.

[3] A. Hessel, M. H. Chen, R. C. Li, and A. A. Oliner, "Propagation in periodically loaded waveguides with higher symmetries," *Proceedings of the IEEE*, vol. 61, no. 2, pp. 183–195, 1973.

[4] P. Crepeau and P. R. McIsaac, "Consequences of symmetry in periodic structures," *Proceedings of the IEEE*, vol. 52, no. 1, pp. 33–43, 1964.

[5] O. Zetterstrom, R. Hamarneh, and O. Quevedo-Teruel, "Experimental validation of a metasurface Luneburg lens antenna implemented with glide-symmetric substrate-integrated holes," *IEEE Antennas and Wireless Propagation Letters*, vol. 20, no. 5, pp. 698–702, 2021.

[6] O. Quevedo-Teruel, J. Miao, M. Mattsson, A. Algaba-Brazalez, M. Johansson, and L. Manholm, "Glide-symmetric fully metallic Luneburg lens for 5G communications at Ka-band," *IEEE Antennas and Wireless Propagation Letters*, vol. 17, no. 9, pp. 1588–1592, 2018.

[7] A. Monje-Real, N. Fonseca, O. Zetterstrom, E. Pucci, and O. Quevedo-Teruel, "Holey glide-symmetric filters for 5G at millimeter-wave frequencies," *IEEE Microwave and Wireless Components Letters*, vol. 30, no. 1, pp. 31–34, 2019.

[8] M. Ebrahimpouri, A. A. Brazalez, L. Manholm, and O. Quevedo-Teruel, "Using glide-symmetric holes to reduce leakage between waveguide flanges," *IEEE Microwave and wireless components letters*, vol. 28, no. 6, pp. 473–475, 2018.

[9] Z. Sipus, K. Cavar, M. Bosiljevac, and E. Rajo-Iglesias, "Glide-symmetric holey structures applied to waveguide technology: design considerations," *Sensors*, vol. 20, no. 23, p. 6871, 2020.

[10] Q. Chen, O. Zetterstrom, E. Pucci, A. Palomares-Caballero, P. Padilla, and O. Quevedo-Teruel, "Glide-symmetric holey leaky-wave antenna with low dispersion for 60 ghz point-to-point communications," *IEEE Transactions on Antennas and Propagation*, vol. 68, no. 3, pp. 1925–1936, 2020.

[11] F. Mesa, G. Valerio, R. Rodriguez-Berral, and O. Quevedo-Teruel, "Simulation-assisted efficient computation of the dispersion diagram of periodic structures: A comprehensive overview with applications to filters, leaky-wave antennas and metasurfaces," *IEEE Antennas and Propagation Magazine*, vol. 63, no. 5, pp. 33–45, 2020.

[12] G. Valerio, F. Ghasemifard, Z. Sipus, and O. Quevedo-Teruel, "Glide-symmetric all-metal holey metasurfaces for low-dispersive artificial materials: Modeling and properties," *IEEE Transactions on Microwave Theory and Techniques*, vol. 66, no. 7, pp. 3210–3223, 2018.

[13] J. T. Vásquez, J. Rivero, G. Valerio, and F. Vipiana, "Periodic integral equation formulation for the numerical analysis of glide structures," in *2022 16th European Conference on Antennas and Propagation (EuCAP)*. IEEE, 2022, pp. 1–3.

[14] J. Rivero, J. T. Vásquez, G. Valerio, and F. Vipiana, "Numerical modelling of glide periodic structures via integral equations," in *2021 15th European Conference on Antennas and Propagation (EuCAP)*. IEEE, 2021, pp. 1–3.

[15] S. Oroskar, D. R. Jackson, and D. R. Wilton, "Efficient computation of the 2D periodic Green's function using the Ewald method," *Journal of Computational Physics*, vol. 219, no. 2, pp. 899–911, 2006.

[16] P. P. Ewald, "Die berechnung optischer und elektrostatischer gitterpotentiale," *Annalen der physik*, vol. 369, no. 3, pp. 253–287, 1921.

[17] C. Linton, "The Green's function for the two-dimensional Helmholtz equation in periodic domains," *Journal of Engineering Mathematics*, vol. 33, no. 4, pp. 377–401, 1998.

[18] F. T. Celepcikay, D. R. Wilton, D. R. Jackson, and F. Capolino, "Choosing splitting parameters and summation limits in the numerical evaluation of 1-D and 2-D periodic Green's functions using the Ewald method," *Radio Science*, vol. 43, no. 06, pp. 1–11, 2008.

[19] M. M. Ney, "Method of moments as applied to electromagnetic problems," *IEEE transactions on microwave theory and techniques*, vol. 33, no. 10, pp. 972–980, 1985.

[20] S. Rao, D. Wilton, and A. Glisson, "Electromagnetic scattering by surfaces of arbitrary shape," *IEEE Transactions on antennas and propagation*, vol. 30, no. 3, pp. 409–418, 1982.

[21] M. A. Khayat, D. R. Wilton, and P. W. Fink, "An improved transformation and optimized sampling scheme for the numerical evaluation of singular and near-singular potentials," *IEEE Antennas and Wireless Propagation Letters*, vol. 7, pp. 377–380, 2008.

[22] F. T. Celepcikay, D. R. Wilton, D. R. Jackson, and W. A. Johnson, "Interpolation of Ewald-accelerated periodic Green's function representations for homogeneous or layered media," *IEEE Transactions on Antennas and Propagation*, vol. 65, no. 5, pp. 2517–2525, 2017.